

# Gambierone, a Ladder-Shaped Polyether from the Dinoflagellate *Gambierdiscus belizeanus*

Inés Rodríguez,<sup>†</sup> Grégory Genta-Jouve,<sup>‡</sup> Carmen Alfonso,<sup>§</sup> Kevin Calabro,<sup>||</sup> Eva Alonso,<sup>†</sup> Jon A. Sánchez,<sup>†</sup> Amparo Alfonso,<sup>†</sup> Olivier P. Thomas,<sup>\*,||</sup> and Luis M. Botana<sup>\*,†</sup>

<sup>†</sup>Universidad de Santiago de Compostela, Departamento de Farmacología, Facultad de Veterinaria, 27002 Lugo, Spain

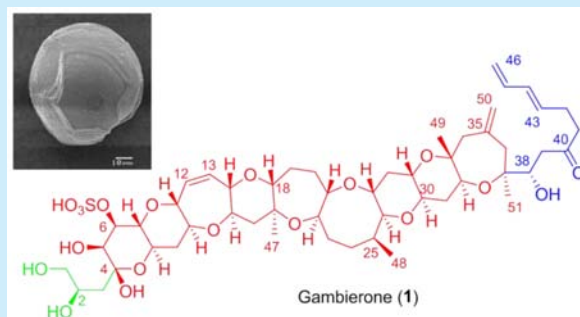
<sup>‡</sup>Université Paris Descartes, Laboratoire de Pharmacognosie et de Chimie des Substances Naturelles, COMETE UMR 8638 CNRS, 4 Avenue de l'Observatoire, 75006 Paris, France

<sup>§</sup>Laboratorio CIFGA S.A., Plaza de Santo Domingo, no. 20, 5a planta, 27001 Lugo, Spain

<sup>||</sup>Université Nice Sophia Antipolis, Institut de Chimie de Nice, UMR 7272 CNRS, Faculté des Sciences, Parc Valrose, 06108 Nice, France

## Supporting Information

**ABSTRACT:** A new natural product named gambierone (**1**) was isolated from the cultured dinoflagellate *Gambierdiscus belizeanus*. The structure of this compound features an unprecedented polyether skeleton and an unusual right-hand side chain. Its relative configuration was fully determined by interpretation of ROESY experiment and comparison between experimental and theoretical NMR data. Although the succession of cycles has no chemical similarity with ciguatoxins, **1** has a molecular formula and biological activity similar to those of CTX-3C, although much lower in intensity.



The increased occurrence of harmful algal blooms is now well documented, and the toxins produced by these microorganisms represent one of the major marine food safety risks. Among the species responsible for the production of toxic substances, the genus *Gambierdiscus* is often involved, mostly in the Pacific Ocean, but also in the Caribbean Sea and Indian Ocean.<sup>1–5</sup> Two major groups of toxins are produced by these ciguatera-causing dinoflagellates: ciguatoxins (CTX), which are the largest cause of fish poisoning,<sup>3</sup> and maitotoxins (MTX), one of the most complex nonpolymeric natural products to date.<sup>6</sup> More recently, smaller but still intricate polyether analogues were identified from some species as exemplified by gambierol, a neuroactive compound,<sup>7–9</sup> gambieric acids,<sup>10,11</sup> and gambieroxide,<sup>12</sup> with a structure similar to that of yessotoxins (YTX). These recent findings underscore the still largely untapped chemical diversity produced by *Gambierdiscus* spp. and encourage further chemical characterization of their specialized metabolome.

Because chemical diversity is undoubtedly linked to variability in the strains or species cultured, we decided to focus on the metabolome of the cultivable species *G. belizeanus* in the search for original polyether architectures. Guided by the presence of ciguatoxin-like compounds (through LC-MS), our chemical study resulted in the isolation and structure elucidation of a new ladder-shaped toxin named gambierone (**1**) (Figure 1). Although the structure is more related to YTX than CTX or MTX, it reveals a new polycyclic ether core as well as original side chains. This compound was further assayed

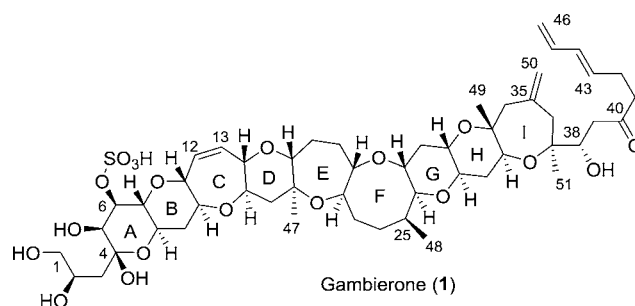


Figure 1. Chemical structure of **1**.

for its biological activity compared with CTX and MTX bioactivities.<sup>13</sup>

Compound **1** was isolated from cultures of *G. belizeanus* (CCMP401) obtained from the Provasoil-Guillard National Center for Marine Algae and Microbiota. The cells were cultured and grown in seawater enriched with modified K medium. The growth was divided in steps, increasing the volume progressively until 20 L. The methanol extracts were then purified through several liquid–liquid partitions, solid phase extractions (SPE), and preparative HPLC coupled to mass detection (see Supporting Information). Compound **1**

Received: March 28, 2015

Published: May 7, 2015

**Table 1.**  $^1\text{H}$  (750 MHz) and  $^{13}\text{C}$  NMR Data in ppm for Gambierone (**1**) in  $\text{CD}_3\text{OD}$

no.	$\delta_{\text{H}}$ , mult. ( $J$ in Hz)	$\delta_{\text{C}}$	no.	$\delta_{\text{H}}$ , mult. ( $J$ in Hz)	$\delta_{\text{C}}$
1	3.47, dd (11.0, 4.5) 3.42, m	67.9	27	3.51, m	77.9
2	4.11, m	70.3	28	2.20, m 1.33, q (11.3)	39.8
3	2.01, m 1.70, dd (14.5, 10.0)	39.6	29	3.12, td (9.5, 4.3)	70.2
4	-	101.0	30	2.94, ddd (11.5, 9.5, 4.5)	78.3
5	4.21, d (3.2)	73.1	31	1.90, m 1.55, q (11.5)	34.9
6	4.70, dd (10.0, 3.2)	77.9	32	3.77, m	72.6
7	3.37, t (10.0)	77.4	33	-	77.4
8	3.77, m	68.0	34	2.35, d (12.0) 2.14, d (12.0)	54.2
9	2.17, m 1.58, q (12.0)	37.8	35	-	144.0
10	3.35, m	79.8	36	2.54, d (14.0) 2.22, d (14.0)	43.3
11	3.79, m	82.6	37	-	80.0
12	5.64, dt (12.5, 2.5)	133.2	38	4.06, dd (8.7, 3.5)	73.5
13	5.75, dt (12.5, 2.5)	133.5	39	2.62, dd (12.0, 3.0) 2.60, dd (12.0, 9.0)	45.8
14	3.81, m	83.2	40	-	212.2
15	3.44, m 1.99, m 1.49, t (11.0)	80.0	41	2.61, t (7.0)	43.7
16	1.49, t (11.0)	47.4	42	2.33, q (7.0)	27.3
17	-	76.7	43	5.70, dt (15.0, 7.0)	134.9
18	3.00, dd (11.0, 2.5) 1.78, m 1.62, m	87.0	44	6.08, dd (15.0, 10.5)	133.4
19	1.62, m	25.3	45	6.29, dt (17.0, 10.4)	138.9
20	1.95, m 1.80, m	34.2	46	5.08, dd (17.0, 1.8) 4.94, dd (10.3, 1.8)	115.9
21	3.54, m	87.6	47	1.20, s	16.2
22	3.54, m	75.9	48	1.00, d (7.3)	13.3
23	1.82, m 1.64, m	32.7	49	1.19, s	16.7
24	1.92, m 1.77, m	29.5	50	4.98, br s 4.86, br s	119.0
25	2.19, m	35.6	51	1.13, s	20.6
26	3.11, m	86.1			

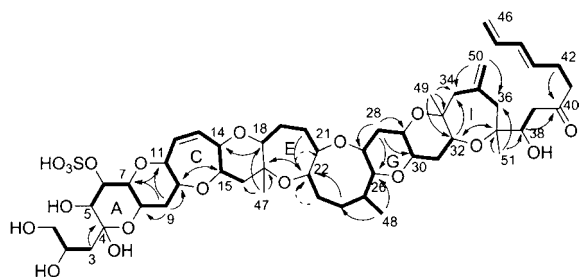


**Figure 2.** Key COSY (bold), H2BC (dotted arrow from H to C), and HMBC (arrow from H to C) correlations for **1**.

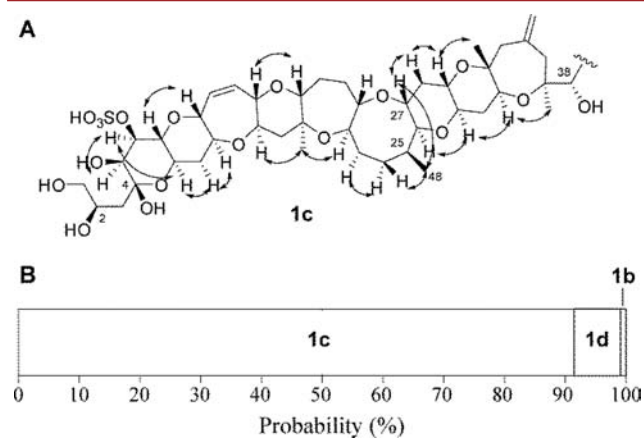


**Figure 3.** Relative configuration for Gambierone (**1**): (A) ROESY (arrows) and (B) DP4 probabilities of the eight diastereoisomers.<sup>17</sup>

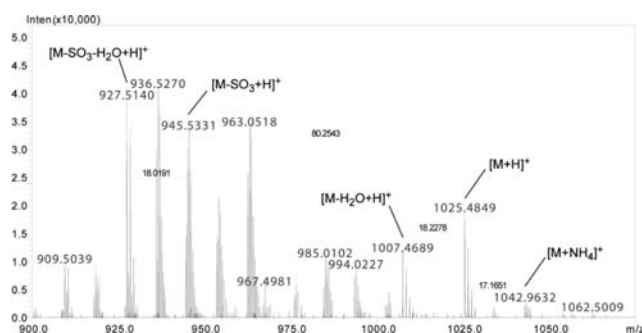


**Figure 4.** Mass spectrum of **1** by LC-MS.

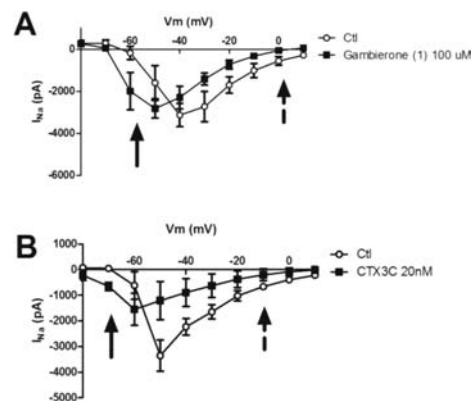


**Figure 5.** Modification of voltage-dependent activation of  $\text{Na}^+$  current ( $I_{\text{Na}}$ ) through  $\text{Na}_v 1.6$  subunits by gambierone (**1**). (A)  $I$ - $V$  curves in the presence and absence of **1** when  $I_{\text{Na}}$  is calculated for each voltage step from  $-100$  to  $20$  mV. (B) Voltage-current relationship in the presence of  $20$  nM CTX<sub>3</sub>C standard where the first continuous arrow showed the earlier activation and the second discontinuous arrow marked the absence of current.

(2.2 mg, 0.012% yield) was purified from the hydrophilic fraction obtained after  $\text{C}_{18}$  SPE.<sup>14</sup>

The molecular formula  $\text{C}_{51}\text{H}_{76}\text{O}_{19}\text{S}$  was deduced from a detailed analysis of the HRMS data with a molecular ion at  $m/z$  1025.4779 ( $[\text{M} + \text{H}]^+$ , calcd 1025.4774) and an isotopic pattern consistent with the presence of one sulfur atom. The planar structure was elucidated with 1.2 mg of pure substance (>98% as estimated both by  $^1\text{H}$  NMR and HPLC-MS), mostly on the basis of 2D NMR data obtained in  $\text{CD}_3\text{OD}$  at 750 MHz (Table 1).

The structure elucidation began with the uncommon right-hand side chain. Indeed, the presence of a conjugated vinyl end was easily deduced from the characteristic signals at  $\delta_{\text{H}}$  5.08 (dd,  $J = 17.0, 2.0$  Hz, H-46a), 4.94 (dd,  $J = 10.5, 2.0$  Hz, H-46b), and 6.29 (dd,  $J = 17.0, 10.5$  Hz, H-45). Based on the chemical shifts of H<sub>2</sub>-41 and C-41 and the presence of a signal at  $\delta_{\text{C}}$  211.4 we suspected a ketone placed at position C-40. Due to overlapping of H<sub>2</sub>-41 and H<sub>2</sub>-39, a clear conclusion could not be given by interpretation of  $^2J_{\text{HC}}$  HMBC coupling but rather based on the H<sub>2</sub>-42 and H-38/C-40  $^3J_{\text{HC}}$  HMBC correlations (Figure 2). The linear right-hand side chain ended with a small second spin coupled system composed of an unusual  $\beta$ -hydroxyketone system. The signals of the C-51 methyl gave key HMBC correlations allowing the connection of the side chain with the polycyclic ring. In addition to the key H<sub>3</sub>-51/C-38 correlation for the side chain, a second H<sub>3</sub>-51/C-36 correlation placed a first AB system on the terminal I ring. As in the case of the second AB system at C-34, these geminal protons are

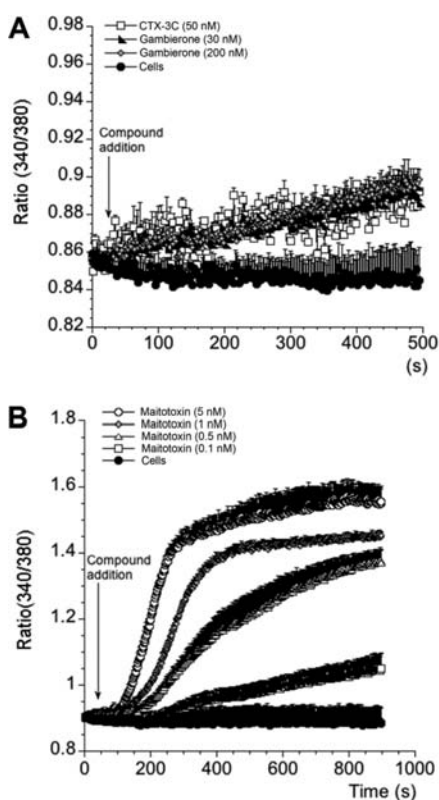


**Figure 6.** Effects of compounds on Fura-2 ratio in SH-SY5Y neuroblastoma cells. SH-SY5Y cells were exposed to (A) 30 nM of CTX-3C standard and two different concentrations (30 and 200 nM) of Gambierone (**1**) or (B) four concentrations of maitotoxin. Mean  $\pm$  SEM of three experiments.

COSY and HMBC correlated with the signals of an *exo* double bond at  $\delta_{\text{H}}$  4.98 (br s, H-50a) and 4.86 (br s, H-50b). Then, a second methyl singlet at  $\delta_{\text{H}}$  1.19 (s, H<sub>3</sub>-49) was used to connect the terminal seven-membered ring with the H-ring. A long spin-coupled system was assigned on the basis of not only COSY but also TOCSY correlations involving the key relay of the signals corresponding to the methyl at C-48. Key H2BC and HMBC correlations allowed us to resolve overlapping of signals H-21 and H-22 at  $\delta_{\text{H}}$  3.54. Indeed,  $^2J_{\text{HC}}$  coupling observed in H2BC between these signals and the signals at  $\delta_{\text{C}}$  75.8 (C-22) and 87.4 (C-21) unambiguously placed the corresponding protons in an adjacent position. HMBC correlations starting from H<sub>3</sub>-47 connected this spin-coupled system to a subsequent polyether spin-coupled system building the last A/B/C rings that includes a double bond on the C-ring. Elucidation of the last A-ring was rendered difficult by the presence of a quaternary carbon at C-4 and the absence of clear HMBC correlations from H-5 and H-6. The nonassigned signal at  $\delta_{\text{C}}$  100.8 (C-4) was reminiscent of a ketal or hemiketal and a gHMBC H<sub>2</sub>-3/C-4 correlation connecting the left-hand side chain to this quaternary carbon. The hemiketal was finally placed at C-4 of the polyether ring to complete the structure. From comparison with the expected molecular formula, the lack of 80 amu and a sulfur atom in our structure led us to assume the presence of a sulfate group substituted on one of the alcohols of the compound. The strong deshielding observed for the signals at  $\delta_{\text{H}}$  4.70 (dd,  $J = 10.0, 3.0$  Hz, H-6) and  $\delta_{\text{C}}$  77.8 (C-6) led us to suggest the location of this sulfate at C-6. This assumption was further confirmed by comparison with the

signals of known compounds of the YTX family frequently exhibiting such substitution.<sup>15</sup>

The determination of the relative configuration around the polycyclic core was mainly based on the ROESY spectrum (Figure 3A). A full *trans*-fused ring system was evidenced and confirmed by some coupling constant values of fused protons. The configuration of the C-48 methyl at C-25 was also deduced from a strong H<sub>3</sub>-48/H-27 NOE. Three undetermined asymmetric centers remained at C-2, C-4, and C-38. Because of the low quantity of compound available we were unable to obtain the relative configurations through chemical derivation. We then turned to <sup>13</sup>C NMR modeling of the eight possible diastereoisomers,<sup>16</sup> and more specifically to the application of a well established calculation of the DP4 probability.<sup>17</sup> After structure optimization of the different diastereoisomers (**1a–1h** see Supporting Information), a probability was assigned to each most stable conformer. Diastereoisomer **1c** was clearly identified as the most probable, as it was assigned a 91.2% confidence (Figure 3B). Therefore, we are able to propose the following relative configurations: 2*R*\*, 4*R*\*, and 38*S*\* for the remaining asymmetric centers. Unfortunately, no clear conclusion could be obtained from the electronic circular dichroism spectra due to the absence of a clear asymmetric chromophore, thus the absolute configuration remains unsolved.

In order to confirm the molecular weight of **1**, an ultrafast liquid chromatography-ion trap/time-of-flight mass spectrometry UPLC-IT-TOF analysis of the pure compound was performed in the positive mode. Compound **1** was shown to follow the typical pattern of ion formation for polyether derivatives, which includes ammonium adducts, water and sulfate losses.<sup>18</sup> Indeed, five characteristic ions were formed at  $m/z$  1025.4849 [ $\text{M} + \text{H}$ ]<sup>+</sup>, 1007.4689 [ $\text{M} - \text{H}_2\text{O} + \text{H}$ ]<sup>+</sup>, 945.5331 [ $\text{M} + \text{H} - \text{SO}_3$ ]<sup>+</sup>, 927.5140 [ $\text{M} + \text{H} - \text{SO}_3 - \text{H}_2\text{O}$ ]<sup>+</sup>, and 1042.9632 [ $\text{M} + \text{NH}_4$ ]<sup>+</sup> (Figure 4). Therefore, compound **1** has a molecular weight of 1024.5 and a mass pattern similar to CTXs.

Since gambierone (**1**) was isolated from a hydrophilic fraction, typical of MTX, we wanted to determine whether the molecule was active in sodium channels (CTX-like effect) or would open calcium pores (MTX-like effect). The biological activity of **1** was tested by electrophysiological measurements in Na<sub>v</sub> 1.6 expressing cells and by checking the effect on cytosolic calcium (Ca<sup>2+</sup>) levels in neuroblastoma cells (SH-SY5Y cell line). Since CTX has proved to cause a hyperpolarizing shift in the voltage dependence of Na<sup>+</sup> channels activation,<sup>19</sup> different concentrations of this new compound were added to the extracellular solution to study its effect over the voltage–current relationship (*I–V* curve). As shown in Figure 5A, compound **1** induces a left shift of the voltage-dependent activation curve at 100  $\mu\text{M}$ . Control cells showed a maximum peak amplitude at  $-40$  mV, and after addition of compound **1**, the peak was shifted negatively to  $-55$  mV. Likewise, CTX-3C also produced a marked hyperpolarization with the corresponding shift of the curve at nanomolar concentrations (Figure 5B). These results demonstrate that **1** promotes the appearance of sodium currents at hyperpolarized potentials in a similar fashion as CTX-3C, although with much less potency.

A small cytosolic Ca<sup>2+</sup> increase has been described in the presence of P-CTX-1 in neuroblastoma and ganglion neurons.<sup>20</sup> This effect was sodium-dependent and was not observed with other CTX analogues. The same effect was observed in IB4-positive neurons.<sup>21</sup> When compound **1** was



added at 30 and 200 nM to SH-SY5Y cells, a slight cytosolic  $\text{Ca}^{2+}$  increase was observed (Figure 6A). The same effect was produced when the CTX-3C standard was used at 50 nM. In both cases the effect was not dose dependent. However, when MTX was added in the medium, a fast cytosolic  $\text{Ca}^{2+}$  increase was observed (Figure 6B) in a dose dependent manner. Therefore, **1** mimics the effect of CTX-3C on cytosolic  $\text{Ca}^{2+}$  currents and does not show any MTX-like effect in calcium levels, hence excluding the possible functional relationship with MTX or analogs.<sup>22</sup>

The biosynthetic pathways of ladder-shape polyethers have been found to imply complex polyketide synthases.<sup>23</sup> While incorporation studies have led to some propositions for brevetoxins and yessotoxins, no experimental data have been reported for CTX or MTX.<sup>24</sup> Comparing the structures of **1** with CTX and MTX did not evidence a clear metabolic link between all these compounds; however, the positions of branched methyls or methylene suggest the involvement of propionate units (see Supporting Information).

## ■ ASSOCIATED CONTENT

### ■ Supporting Information

Detailed experimental procedures; NMR, MS, and ECD data; procedure for configurational assignment; biosynthetic hypothesis. The Supporting Information is available free of charge on the ACS Publications website at DOI: 10.1021/acs.orglett.5b00902.

## ■ AUTHOR INFORMATION

### ■ Corresponding Authors

\*E-mail: Olivier.thomas@unice.fr.

\*E-mail: Luis.Botana@usc.es.

### ■ Notes

The authors declare no competing financial interest.

## ■ ACKNOWLEDGMENTS

Inès Rodriguez was supported by a fellowship from Subprograma de Formación de Personal Investigador (AGL2012-40185-CO2-01), Spain. This research received funding from the following FEDER cofunded grants from CDTI and Technological Funds, supported by Ministerio de Economía y Competitividad, AGL2012-40185-CO2-01, and Consellería de Cultura, Educación e Ordenación Universitaria, GRC2013-016, and through Axencia Galega de Innovación, Spain, ITC-20133020 SINTOX, and funding from the European Union's Seventh Framework Programme managed by REA – Research Executive Agency (FP7/2007-2013) under Grant Agreement 315285 CIGUATOOLS and 312184 PHARMASEA. This work was granted access to the HPC resources of IDRIS under the allocation 2014-100483 OUMOLPO made by GENCI. The authors thank the Ciguatools consortium for their support in this work.

## ■ REFERENCES

- (1) Michael, J. H.; Andreas, B.; Richard, J. L. *Dinoflagellate Toxins*. In *Seafood and Freshwater Toxins*; Botana, L. M., Ed.; CRC Press: Boca Raton, FL, 2014; pp 3–38.
- (2) Parsons, M. L.; Aligizaki, K.; Bottein, M.-Y. D.; Fraga, S.; Morton, S. L.; Penna, A.; Rhodes, L. *Harmful Algae* **2012**, *14*, 107–129.
- (3) Alexander, J.; Benford, D.; Boobis, A.; Ceccatelli, S.; Cravedi, J.-P.; Di Domenico, A.; Doerge, D.; Dogliotti, E.; Edler, L.; Farmer, P.; Filipic, M.; Fink-Gremmels, J.; Furst, P.; Guerin, T.; Knutsen, H. K.

Machala, M.; Mutti, A.; Schlatter, J.; van Leeuwen, R.; Botana, L.; Heinemeyer, G.; Hess, P.; Preiss-Weigert, A.; van Egmond, H.; Eskola, M.; Vernazza, F. *EFSA J.* **2010**, *8* (1627), 1638.

(4) Nicholson, G. M.; Lewis, R. J. *Mar. Drugs* **2006**, *4*, 82–118.

(5) Litaker, R. W.; Vandersea, M. W.; Faust, M. A.; Kibler, S. R.; Nau, A. W.; Holland, W. C.; Chinain, M.; Holmes, M. J.; Tester, P. A. *Toxicon* **2010**, *56*, 711–730.

(6) Martin, V.; Vale, C.; Antelo, A.; Hiram, M.; Yamashita, S.; Vieytes, M. R.; Botana, L. M. *Chem. Res. Toxicol.* **2014**, *27*, 1387–1400.

(7) Kopljar, I.; Labro, A. J.; Cuypers, E.; Johnson, H. W. B.; Rainier, J. D.; Tytgat, J.; Snyders, D. J. *Proc. Natl. Acad. Sci. U.S.A.* **2009**, *106* (9896–9901), S9896/9891–S9896/9898.

(8) Satake, M.; Murata, M.; Yasumoto, T. *J. Am. Chem. Soc.* **1993**, *115*, 361–362.

(9) Alonso, E.; Fuwa, H.; Vale, C.; Suga, Y.; Goto, T.; Konno, Y.; Sasaki, M.; LaFerla, F. M.; Vieytes, M. R.; Gimenez-Llort, L.; Botana, L. M. *J. Am. Chem. Soc.* **2012**, *134*, 7467–7479.

(10) Nagai, H.; Murata, M.; Torigoe, K.; Satake, M.; Yasumoto, T. *J. Org. Chem.* **1992**, *57*, 5448–5453.

(11) Nagai, H.; Torigoe, K.; Satake, M.; Murata, M.; Yasumoto, T.; Hirota, H. *J. Am. Chem. Soc.* **1992**, *114*, 1102–1103.

(12) Watanabe, R.; Uchida, H.; Suzuki, T.; Matsushima, R.; Nagae, M.; Toyohara, Y.; Satake, M.; Oshima, Y.; Inoue, A.; Yasumoto, T. *Tetrahedron* **2013**, *69*, 10299–10303.

(13) Botana, L. M., Guide to Phycotoxin Monitoring of Bivalve Mollusk-Harvesting Areas. In *Seafood and Freshwater Toxins*; Botana, L. M., Ed.; CRC Press: Boca Raton, FL, 2014; pp 39–56.

(14) Colorless amorphous solid;  $[\alpha]_{20}^D = -17$  (c 0.05, MeOH);  $\lambda_{\text{max}}$  (log  $\epsilon$ ), 226 (4.7), 202 (5.0) nm; IR (ATR)  $\nu_{\text{max}}$  3475, 2960, 2870, 1720  $\text{cm}^{-1}$ ; for  $^1\text{H}$  and  $^{13}\text{C}$  NMR data in  $\text{CD}_3\text{OD}$ , see Table 1; HRESIMS  $m/z$   $[\text{M} + \text{H}]^+$  1025.4779 (calcd for  $\text{C}_{51}\text{H}_{77}\text{O}_{19}\text{S}$ , 1025.4774).

(15) Paz, B.; Daranas, A. H.; Norte, M.; Riobo, P.; Franco, J. M.; Fernandez, J. J. *Mar. Drugs* **2008**, *6*, 73–102.

(16) Willoughby, P. H.; Jansma, M. J.; Hoye, T. R. *Nat. Protoc.* **2014**, *9*, 643–660.

(17) Smith, S. G.; Goodman, J. M. *J. Am. Chem. Soc.* **2010**, *132*, 12946–12959.

(18) Otero, P.; Perez, S.; Alfonso, A.; Vale, C.; Rodriguez, P.; Gouveia, N. N.; Gouveia, N.; Delgado, J.; Vale, P.; Hiram, M.; Ishihara, Y.; Molgo, J.; Botana, L. M. *Anal. Chem.* **2010**, *82*, 6032–6039.

(19) Perez, S.; Vale, C.; Botana, A. M.; Alonso, E.; Vieytes, M. R.; Botana, L. M. *Chem. Res. Toxicol.* **2011**, *24*, 1153–1157.

(20) Molgo, J.; Shimahara, T.; Gaudry-Talarmin, Y. M.; Comella, J. X.; Legrand, A. M. *Bull. Soc. Pathol. Exot.* **1992**, *85*, 486–488.

(21) Irina, V.; Katharina, Z.; Richard, J. L., Ciguatera Toxins. In *Seafood and Freshwater Toxins*; Botana, L. M., Ed.; CRC Press: Boca Raton, FL, 2014; pp 925–950.

(22) Holmes, M. J.; Lewis, R. J.; Gillespie, N. C. *Toxicon* **1990**, *28*, 1159–1172.

(23) Kellmann, R.; Stüken, A.; Orr, R. J. S.; Svendsen, H. M.; Jakobsen, K. S. *Mar. Drugs* **2010**, *8*, 1011–1048.

(24) Calabro, K.; Guignonis, J.-M.; Teyssié, J.-L.; Oberhänsli, F.; Goudour, J.-P.; Warnau, M.; Bottein, M.-Y.; Thomas, O. *Toxins* **2014**, *6*, 1785–1798.